KINETIC THEORY OF REACTIVE GAS MIXTURES WITH APPLICATION TO COMBUSTION

Alexandre Ern[1] and Vincent Giovangigli[2]

[1] CERMICS, Ecole Nationale des Ponts et Chaussées, F-77455 Marne la Vallée cedex 2, France
[2] CMAP, Ecole Polytechnique, F-91128 Palaiseau cedex, France

Abstract. We consider a generalized Boltzmann equation for dilute isotropic gas mixtures with chemical reactions. Depending on the ratio of characteristic times between reactive and inert collisions, various chemical regimes are obtained in the first order Enskog expansion and their compatibility with Boltzmann's H-theorem is investigated. We then review the mathematical structure of the transport linear systems obtained from a Galerkin approximation of the integral equations for the species perturbed distribution functions. In the framework of this theory, the multicomponent transport coefficients are written as convergent series and accurate approximate expressions are obtained by truncation. Numerical results are presented for various combustion applications including laminar flame propagation, counterflow flame extinction and multidimensional bunsen flames.

1 INTRODUCTION

Chemically reactive gas mixtures arise in several applications including combustion engines, industrial or commercial burners, chemical reactors, spacecraft flights and plasma physics. In most of these applications, the kinetic theory of reactive gas mixtures may improve the fundamental understanding of the macroscopic phenomena involved and also enhance accuracy and robustness of the numerical models used by engineers. In this work, we are concerned with dilute isotropic gas mixtures. We consider an arbitrary number of chemical species having internal degrees of freedom and participating in an arbitrary number of chemical reactions. With an eye towards combustion applications, our goal is to address some physical, mathematical and numerical aspects of the kinetic theory of reactive gas mixtures and the associated Navier-Stokes regime obtained in the first order Enskog expansion.

In Section 2, we investigate a reactive Boltzmann equation and the first order Enskog expansion. The kinetic theory of inert, dilute, isotropic, polyatomic gas mixtures has been derived in [1] in a semiclassical framework, i.e. translational motion was treated classically and internal degrees of freedom were treated quantum mechanically. We also refer to classical textbooks on kinetic theory [2–4]. The Boltzmann equations derived in [1] can be generalized to reactive gas mixtures by considering an additional reactive source term introduced in [5] and further investigated in [6–11].

Both the inert and the reactive source terms yield a positive contribution to the kinetic entropy production at the microscopic level. Depending on the ratio of characteristic times between reactive and inert collisions, various chemical regimes can be obtained in the first order Enskog expansion. The kinetic chemical equilibrium regime, based on the assumption that both characteristic times are of the same order of magnitude, has been introduced in [5] and further investigated in [10] where, in particular, it was shown that this regime was compatible with Boltzmann's H-theorem. On the other hand, the Maxwellian reaction regime, recovered for large characteristic time ratios, is also compatible with Boltzmann's H-theorem. In several applications, the previous assumptions on characteristic times are not met and one may consider an intermediate regime in which the first order macroscopic equations contain two additional terms with respect to the Maxwellian reaction regime: a chemical pressure first pointed out in [5] and a perturbation to the chemistry source term [5,8,12]. However, as detailed below, these perturbations do not yield positive entropy production. Since several estimates [12–18] indicate that these perturbations are generally small, combustion applications will be modeled using the Maxwellian reaction regime.

In Section 3, we investigate the mathematical structure of the transport linear systems. These systems result from a Galerkin approximation of the integral equations satisfied by the species perturbed distribution functions. The mathematical structure only relies on the dissipative nature of inelastic collisions and some simple properties of the variational space selected to approximate the species perturbed distribution functions [8,19]. In particular, it is valid independently of the particular form of the transition probabilities or the intermolecular potentials. As a direct consequence of the mathematical structure, it is shown that the multicomponent transport coefficients may be expanded as convergent series. Cost effective and accurate approximations are then obtained by truncation [20].

Finally, in Section 4, we present numerical results illustrating the impact of multicomponent transport modeling on combustion phenomena, including laminar flame propagation, counterflow flame extinction and multidimensional bunsen flames. We focus on the Soret effect associated with species diffusion due to temperature gradients. Although this effect may impact flame structures because it plays an important role in the mass balance of active radicals such as H, O and OH near the flame front, it has seldom been accounted for in combustion applications. One reason for that was the extremely high computational cost involved with the evaluation of thermal diffusion coefficients. The algorithms presented in this paper are much more cost effective and thus enable the combustion scientist to quantify the role played by the Soret effect in several flame structures.

2 KINETIC THEORY OF REACTIVE GAS MIXTURES

In this section, we present a generalized Boltzmann equation valid for dilute polyatomic gas mixtures with chemical reactions and investigate some properties of the first order Enskog expansion, in particular the compatibility with Boltzmann's H-theorem. For the sake of simplicity, the analysis is restricted to isotropic gas mixtures, thus excluding for instance the presence of strong external magnetic fields.

2.1 Reactive Boltzmann equations

We consider a dilute isotropic reactive gas mixture with n chemical species having internal degrees of freedom. The state of the mixture is described by the species distribution functions $f_i(t, x, c_i, I)$ where t is the time, x the three-dimensional spatial coordinate, c_i the velocity of the ith species and I the index for internal energy states. For a family of functions ζ_i only depending on c_i and I, we use the notation $\zeta = (\zeta_i)_{i \in S}$ where $S = [1, n]$. We introduce the scalar product

$$\langle\langle \xi, \zeta \rangle\rangle = \sum_{\substack{i \in S \\ I \in Q_i}} \int \xi_i \, \zeta_i \, dc_i,$$

where Q_i is the set of quantum state indices for the ith species. Let also $\mathcal{I}$ be the space spanned by the $n + 4$ collisional invariants associated with species, momentum and energy

$$\begin{cases} \psi^k = (\delta_{ki})_{i \in S}, & k \in S, \\ \psi^{n+\nu} = (m_i c_{\nu i})_{i \in S}, & \nu = 1, 2, 3, \\ \psi^{n+4} = (\frac{1}{2} m_i c_i^2 + E_{iI})_{i \in S}, \end{cases}$$

where δ_{ki} is the Kronecker symbol, m_i the mass of the ith species, $c_{\nu i}$ the νth coordinate of c_i and E_{iI} the energy of internal state I for the ith species.

The family of species distribution functions $f = (f_i)_{i \in S}$ is the solution of generalized Boltzmann equations in the form

$$\mathcal{D}_i(f_i) = \mathcal{S}_i(f) + \mathcal{C}_i(f), \quad i \in S, \tag{1}$$

where $\mathcal{D}_i(f_i)$ is the usual streaming differential operator, $\mathcal{S}_i(f)$ the scattering source term and $\mathcal{C}_i(f)$ the chemistry source term. The scattering source term has been derived in [1] for dilute, inert, isotropic, polyatomic gas mixtures and reads

$$\mathcal{S}_i(f) = \sum_{j \in S} \sum_{\substack{J \in Q_j \\ I' \in Q_i \\ J' \in Q_j}} \int (f_i' f_j' \frac{a_{iI} a_{jJ}}{a_{iI'} a_{jJ'}} - f_i f_j) W_{ij}^{IJI'J'} \, dc_j dc_i' dc_j', \tag{2}$$

where primes denote values after collision, a_{iI} the degeneracy of the Ith quantum energy shell of the ith species and $W_{ij}^{IJI'J'}$ the transition probability for an inert collision between species pair (i, j) going from energy states (I, J) to energy states (I', J'). The transition probabilities satisfy the reciprocity relations $W_{ij}^{IJI'J'} a_{iI} a_{jJ} = W_{ij}^{I'J'IJ} a_{iI'} a_{jJ'}$. The scattering source term satisfies $\langle\langle \psi^l, \mathcal{S}(f) \rangle\rangle = 0$ for $1 \leq l \leq n + 4$, yielding the macroscopic conservation equations in the form

$$\langle\langle \psi^l, \mathcal{D}(f) \rangle\rangle = \langle\langle \psi^l, \mathcal{C}(f) \rangle\rangle, \quad 1 \leq l \leq n + 4.$$

Since chemical reacions conserve momentum and energy, we have $\langle\langle \psi^l, \mathcal{C}(f) \rangle\rangle = 0$ for $n+1 \leq l \leq n+4$. The chemistry source term is also orthogonal to the atomic invariants $(n_{ia})_{i \in S}$ where n_{ia} is the number of atoms a in species i.

We consider a chemical mechanism with an arbitrary number of elementary reactions. Although triple nonreactive collisions have been neglected in the scattering source term, the chemistry source term involves bimolecular and trimolecular reactions. The latter are indeed important in several applications since recombination reactions cannot often proceed otherwise [6,9,10]. Elementary reactions are written in the form $\sum_{j\in S_r^f}\chi_j \rightleftharpoons \sum_{k\in S_r^b}\chi_k$ for $r\in R$, where S_r^f and S_r^b are, respectively, the index sets in the forward and backward reaction and R the indexing set for reactions. Indices in S_r^f and S_r^b are counted with their order of multiplicity. We adopt the notational convention that an index set with a subscript in parenthesis means that the index has been removed only once from this set. The reactive source term for the ith species may then be written as $\mathcal{C}_i(f)=\sum_{r\in R}\mathcal{C}_i^r(f)$ where

$$\begin{aligned}\mathcal{C}_i^r(f) = \nu_{ir}^f \sum_{F_{r(I)},B_r}\int\Big(\prod_{k\in S_r^b} f_k \frac{\prod_{k\in S_r^b}\beta_{kK}}{\prod_{j\in S_r^f}\beta_{jJ}} - \prod_{j\in S_r^f} f_j\Big)\mathcal{W}_{S_r^f S_r^b}^{F_r B_r}\prod_{j\in S_{r(i)}^f} dc_j \prod_{k\in S_r^b} dc_k \\ + \nu_{ib}^b \sum_{F_r,B_{r(I)}}\int\Big(\prod_{j\in S_r^f} f_j - \frac{\prod_{k\in S_r^b}\beta_{kK}}{\prod_{j\in S_r^f}\beta_{kK}}\prod_{k\in S_r^b} f_k\Big)\mathcal{W}_{S_r^f S_r^b}^{F_r B_r}\prod_{j\in S_r^f} dc_j \prod_{k\in S_{r(i)}^b} dc_k,\end{aligned} \tag{3}$$

where ν_{ir}^f and ν_{ir}^b are the stoichiometric coefficient of the ith species in the rth elementary reaction, $\beta_{iI}=h_P^3/(a_{iI}m_i^3)$ and h_P is the Planck constant. Furthermore, $\mathcal{W}_{S_r^f S_r^b}^{F_r B_r}$ denotes the transition probability for a reactive collision in which the reactants S_r^f with internal energy states F_r are transformed into products S_r^b with internal energy states B_r. The reactive transition probabilities satisfy the reciprocity relations

$$\mathcal{W}_{S_r^f S_r^b}^{F_r B_r}\prod_{k\in S_r^b}\beta_{kK} = \mathcal{W}_{S_r^b S_r^f}^{B_r F_r}\prod_{j\in S_r^f}\beta_{jJ}.$$

For bimolecular reactions, these transition probabilities may be expressed in terms of reactive collision cross-sections but the link between both formalisms is more complex for three body reactions. Conservation of atomic elements, mass, momentum and energy is taken into account using Dirac delta functions in the transition probabilities [5,7,9]. As a simple illustration, the source term for a bimolecular reaction $\chi_i+\chi_j\rightleftharpoons\chi_k+\chi_l$ reads

$$\mathcal{C}_i^r(f) = \sum_{\substack{J\in Q_j\\K\in Q_k\\L\in Q_l}}\int\Big(f_k f_l\frac{\beta_{kK}\beta_{lL}}{\beta_{iI}\beta_{jJ}} - f_i f_j\Big)\mathcal{W}_{ijkl}^{IJKL} dc_j dc_k dc_l.$$

Further examples are given in [10].

A fundamental aspect of the kinetic theory of gases is Boltzmann's H-theorem. The kinetic entropy is defined as

$$\mathcal{E} = -k_B\sum_{\substack{i\in S\\I\in Q_i}}\int f_i(\log(\beta_{iI}f_i)-1)\,dc_i,$$

where k_B is the Boltzmann constant. The source term in the kinetic entropy conservation equation σ may be split into an inert and a reactive contribution

$$\sigma = \sigma^{\mathcal{S}} + \sigma^{\mathcal{C}},$$

with $\sigma^{\mathcal{S}} = -k_B \sum_{\substack{i \in S \\ I \in Q_i}} \int \mathcal{S}_i(f) \log(\beta_{iI} f_i)\, dc_i$, $\sigma^{\mathcal{C}} = -k_B \sum_{\substack{i \in S \\ I \in Q_i}} \int \mathcal{C}_i(f) \log(\beta_{iI} f_i)\, dc_i$. A straightforward calculation yields

$$\sigma^{\mathcal{S}} \geq 0 \quad \text{and} \quad \sigma^{\mathcal{C}} \geq 0,$$

showing that the scattering and reactive source terms are compatible with the H-theorem. Since both contributions are nonnegative independently, particle collisions always increase entropy regardless of the reactive aspect.

2.2 Chemical regimes in the Enskog expansion

We now seek an approximate solution to the generalized Boltzmann equations (1) in the framework of the Enskog expansion [2–4]. We rewrite (1) as

$$\mathcal{D}_i(f_i) = \frac{1}{\varepsilon} \mathcal{S}_i(f) + \varepsilon^a \mathcal{C}_i(f), \quad i \in S, \tag{4}$$

where ε is the formal expansion parameter and a depends on the chemical regime under consideration.

The case $a = -1$ corresponds to the kinetic equilibrium regime in which chemsitry characteristic times are of the same order as inert collision times. This regime has been introduced formally in [5] and further investigated in [10]. Both the zero and first order macroscopic equations (Euler and Navier-Stokes regimes) express conservation of atom densities (as opposed to chemical species), momentum and energy. Furthermore, the entropy source term in the Navier-Stokes regime is shown to be nonnegative [10]. The kinetic chemical equilibrium regime will not be further discussed here and we refer to [10] for more details regarding in particular multicomponent transport coefficients.

We now discuss the chemical regimes associated with $a = 0$ and $a = 1$, termed respectively the strong reaction regime and the Maxwellian reaction regime. Expanding the species distribution functions in the form

$$f_i = f_i^0 \big(1 + \varepsilon \phi_i + O(\varepsilon^2)\big),$$

one readily sees that $\mathcal{S}_i(f^0) = 0$ for $i \in S$ showing that $f^0 = (f_i^0)_{i \in S}$ are Maxwellian distribution functions. The zero order macroscopic equations read

$$\langle\!\langle \psi^l, \mathcal{D}(f^0) \rangle\!\rangle = \delta_{a0} \langle\!\langle \psi^l, \mathcal{C}(f^0) \rangle\!\rangle, \quad 1 \leq l \leq n+4,$$

and express conservation of species mass for $1 \leq l \leq n$, momentum for $n+1 \leq l \leq n+3$ and energy for $l = n+4$. The species source term only arises in the strong reaction regime which yields the reactive Euler equations whereas the inert Euler equations $\langle\!\langle \psi^l, \mathcal{D}(f^0) \rangle\!\rangle = 0$, $1 \leq l \leq n+4$, are recovered for the Maxwellian reaction regime.

Introducing the linearized scattering operator $\mathcal{L}^{\mathcal{S}}$

$$\mathcal{L}_i^{\mathcal{S}}(\zeta) = \sum_{j\in S} \sum_{\substack{J\in Q_j \\ I'\in Q_i \\ J'\in Q_j}} \int f_j^0(\zeta_i + \zeta_j - \zeta_i' - \zeta_j') W_{ij}^{IJI'J'}\, dc_j dc_i' dc_j',$$

we define the integral bracket operator as

$$[\![\xi, \zeta]\!] = \langle\langle f^0 \xi, \mathcal{L}^{\mathcal{S}}(\zeta)\rangle\rangle.$$

It is well known that this operator is symmetric $[\![\xi, \zeta]\!] = [\![\zeta, \xi]\!]$, positive $[\![\xi, \xi]\!] \geq 0$ and its kernel is spanned by the collisional invariants, i.e. $[\![\xi, \xi]\!] = 0$ if and only if $\xi \in \mathcal{I}$. The first order perturbation $\phi = (\phi_i)_{i\in S}$ is then shown to be the solution of constrained integral equations in the form

$$\begin{cases} \mathcal{L}_i^{\mathcal{S}}(\phi) = -\mathcal{D}_i(f_i^0)/f_i^0 + \delta_{a0}\mathcal{C}_i(f^0)/f_i^0, \quad i \in S, \\ \langle\langle f^0\phi, \psi^l\rangle\rangle = 0, \quad 1 \leq l \leq n+4. \end{cases} \tag{5}$$

One can show that ϕ can be written in the form $\phi = \phi^{\mathcal{S}} + \delta_{a0}\phi^{\mathcal{C}}$ with obvious notation. The first order macroscopic equations read

$$\langle\langle \psi^l, \mathcal{D}(f^0) + \mathcal{D}(f^0\phi^{\mathcal{S}}) + \delta_{a0}\mathcal{D}(f^0\phi^{\mathcal{C}})\rangle\rangle = \langle\langle \psi^l, \mathcal{C}(f^0) + \delta_{a0}\partial_f\mathcal{C}(f^0)f^0\phi\rangle\rangle, \quad 1 \leq l \leq n+4.$$

In the left member, the first term corresponds to the Euler fluxes, the second to the inert Navier-Stokes fluxes and the third to a chemistry perturbation of the Navier-Stokes fluxes. This last term yields an additional chemical pressure in the macroscopic pressure tensor [5,8,11]. In the right member, the first term corresponds to the chemistry source term evaluated from Maxwellian distributions and is compatible with the law of mass action while the second term, which is only present in the strong reaction regime, is a perturbation due to the chemistry source term $\mathcal{C}_i(f^0)$. In terms of macroscopic variables, this perturbation is the sum of a polynomial in the species number densities n_i, $i \in S$, of degree lower than $2n_R$ plus a polynomial in n_i, $i \in S$, of degree lower than n_R multiplied by the divergence of the hydrodynamic velocity, where n_R is the maximum number of reactants in reactive collisions (typically 2 or 3). The perturbed terms are discussed in [12] for monatomic species and in [5,8,11] for polyatomic species.

At second order, the kinetic entropy is given by [21]

$$\mathcal{E} = -k_B \sum_{\substack{i\in S \\ I\in Q_i}} \int f_i^0(\log(\beta_{iI} f_i^0) - 1)\, dc_i + O(\varepsilon^2).$$

An asymptotic expression of the entropy source term is obtained by expanding the scattering and reactive source terms yielding

$$\begin{cases} \sigma^{\mathcal{S}} = \varepsilon^{-1}\sigma_{-1}^{\mathcal{S}} + \varepsilon^0\sigma_0^{\mathcal{S}} + \varepsilon^1\sigma_1^{\mathcal{S}} + O(\varepsilon^2), \\ \sigma^{\mathcal{C}} = \varepsilon^0\sigma_0^{\mathcal{C}} + \varepsilon^1\sigma_1^{\mathcal{C}} + O(\varepsilon^2). \end{cases}$$

In the Maxwellian reaction regime where $a = 1$, one easily finds that

$$\sigma_{-1}^{\mathcal{S}} = \sigma_0^{\mathcal{S}} = \sigma_0^{\mathcal{C}} = 0, \quad \sigma_1^{\mathcal{S}} \geq 0, \quad \sigma_1^{\mathcal{C}} \geq 0.$$

As a result, both inert and reactive contributions are nonnegative and have the same order of magnitude. On the other hand, in the strong reaction regime where $a = 0$, only $\sigma_{-1}^{\mathcal{S}}$ and $\sigma_0^{\mathcal{S}}$ vanish, but the reactive contribution $\sigma_0^{\mathcal{C}} + \sigma_1^{\mathcal{C}}$ has no clear sign, in contradiction with the underlying kinetic framework.

In the rest of this work, we focus on the regime $a = 1$ or, equivalently, on the regime $a = 0$ with the chemical pressure and the perturbation of the chemistry source term neglected. This latter assumption is in agreement with estimates published in the literature [12–18]. In terms of macroscopic variables, the Navier-Stokes equations read

$$\partial_t(\rho_i) + \nabla\cdot(\rho_i v) + \nabla\cdot(\rho_i V_i) = \omega_i, \quad i \in S,$$

$$\partial_t(\rho v) + \nabla\cdot(\rho v \otimes v + pI) + \nabla\cdot\Pi = \sum_{i\in S} b_i,$$

$$\partial_t(\rho e) + \nabla\cdot((\rho e + p)v) + \nabla\cdot(Q + \Pi v) = \sum_{i\in S} b_i\cdot(v + V_i),$$

where ρ_i is the density of the ith species, V_i its diffusion velocity, ω_i its mass production rate, v the hydrodynamic flow velocity, $\rho = \sum_{i\in S}\rho_i$ the mixture density, p the pressure, Π the pressure tensor, b_i the external force acting on the ith species, e the specific total energy and Q the heat flux. The multicomponent transport fluxes V_i, Q and Π depend linearly on the macroscopic variable gradients in the form

$$\begin{cases} V_i = -\displaystyle\sum_{j\in S} D_{ij}(d_j + \chi_j \nabla \log T), \quad i \in S, \\ Q = -\lambda\nabla T - p\displaystyle\sum_{j\in S}\chi_j V_j + \sum_{j\in S} H_j V_j, \\ \Pi = -\eta(\nabla v + \nabla v^t - \frac{2}{3}(\nabla\cdot v)I) - \kappa(\nabla\cdot v)I, \end{cases}$$

with $d_j = (\nabla p_j - b_j)/p$, p_j being the partial pressure of the jth species, H_j its volumetric enthalpy and T the temperature. The multicomponent transport coefficients are the diffusion matrix $D = (D_{ij})_{i,j\in S}$ which is symmetric by construction, the thermal diffusion ratios $\chi = (\chi_i)_{i\in S}$, the thermal conductivity λ, the shear viscosity η and the volume viscosity κ. These coefficients depend on the solution of the constrained integral equations (5). The positivity of the entropy source term $\sigma_1^{\mathcal{S}}$ implies that

$$\kappa \geq 0, \quad \eta > 0, \quad \lambda > 0,$$

$$\forall x = (x_1, \ldots, x_n), \qquad (Dx, x) \geq 0 \quad \text{and} \quad \big((Dx, x) = 0 \Longleftrightarrow x = c(\rho_1, \ldots, \rho_n)\big).$$

3 TRANSPORT LINEAR SYSTEMS

3.1 Mathematical structure

An approximate solution of the constrained integral equations (5) is sought in a finite dimensional functional space

$$\mathcal{A} = \text{span}\{\ \xi^{rk}, (r,k) \in B\ \},$$

spanned by Laguerre-Sonine polynomials in the translational energy and Wang Chang and Uhlenbeck polynomials in the internal energy. B is the set of function indices depending on the energy mode r and species k. Using a standard Galerkin method, (5) is transformed in a constrained singular system in the form

$$\begin{cases} G\alpha = \beta, \\ \alpha \in C, \end{cases} \tag{6}$$

where G is a matrix of size ω, α and β are vectors and C is a vector space, typically of dimension 0 or 1. In the first case, the matrix G is nonsingular and in the second case it has a one-dimensional nullspace. A generic transport coefficient μ is then given by the scalar product of the solution vector α with a given vector β'

$$\mu = \langle \alpha, \beta' \rangle,$$

The transport linear system (6) has several important mathematical properties which are now briefly reviewed. For more details we refer to [19]. All the following properties are directly deduced from the kinetic theory framework. They are also independent of the particular form of the transition probabilities or the interaction potentials of the molecules.

As a direct consequence of the properties of the bracket operator, we first deduce that G is symmetric positive semidefinite and positive definite on C and that the vector β is in the range of G. Furthermore, the transport linear system (6) admits a unique solution if and only if the following perpendicularity property holds

$$\mathcal{I} = \mathcal{I} \cap \mathcal{A} \ \oplus\ \mathcal{I} \cap \mathcal{A}^{\perp}.$$

In addition, we point out that the symmetry of G, which is a simple and natural consequence of the kinetic framework, is important mathematically and numerically. However, several authors have destroyed artificially this natural symmetry [22,23].

With an eye toward iterative methods to solve approximately the transport linear systems, we introduce the sparse transport matrix $db(G)$ which only retains couplings between energy modes for each species

$$db(G)^{rs}_{kl} = G^{rs}_{kl}\delta_{kl}, \quad (r,k),\ (s,l) \in B.$$

For instance, when the index r takes two possible values, the matrix G consists of four blocks. Assuming for simplicity that these blocks are of size n, we have

$$db(G) = \begin{pmatrix} \begin{pmatrix} \ddots & 0 \\ 0 & \ddots \end{pmatrix} & \begin{pmatrix} \ddots & 0 \\ 0 & \ddots \end{pmatrix} \\ \begin{pmatrix} \ddots & 0 \\ 0 & \ddots \end{pmatrix} & \begin{pmatrix} \ddots & 0 \\ 0 & \ddots \end{pmatrix} \end{pmatrix}.$$

The sparse transport matrix $db(G)$ has important mathematical properties: the matrix $2db(G) - G$ is symmetric positive definite for $n \geq 3$ and the matrix $db(G)$ is symmetric positive definite for $n \geq 2$. These results are valid assuming the perpendicularity property and the following two assumptions:

- species localization property

$$\forall \xi^{rk} \in \mathcal{A}, \quad \xi_l^{rk} = 0 \text{ for } k \neq l,$$

- species orthogonality property

$$\forall l \in S, \quad \psi^l \in \mathcal{A}^{\perp}.$$

As shown in [19], these 3 assumptions are met for the classical choices of the functional space $\mathcal{A}$.

3.2 Efficient algorithms for numerical evaluation

The mathematical structure of the transport linear systems derived in the previous section leads to fast and accurate algorithms for multicomponent transport property evaluation [20]. Indeed, using the sparse transport matrix $db(G)$, the transport coefficients can be expanded as convergent series which yield approximate expressions by truncation.

A first family of algorithms relies on standard or projected relaxation methods. Letting $M = db(G)$, $T = I - M^{-1}G$ and $P = P_{C,N(G)}$ the linear projector onto the contraint space C parallel to the nullspace $N(G)$ of G, one obtains the approximate expression

$$\mu_{[i]} = \langle \sum_{j=0}^{i} (PT)^j PM^{-1}P^t \beta, \beta' \rangle.$$

Convergence of this series directly results from the fact that $2db(G) - G$ is positive definite. A second family of algorithms uses the conjugate gradient method with the sparse transport matrix $db(G)$ serving as preconditioner. Note that the symmetry of the system matrix G is essential in the conjugate gradient method.

In addition to truncated iterative methods, it may be interesting in some situations to consider a direct numerical inversion of the transport linear system. In this case, the most computationally effective strategy consists in using the symmetric positive semidefinite form of the transport linear system. Introducing appropriate symmetric

rank one perturbations of the system matrix [20], it is then possible to perform a direct numerical inversion at half the cost with respect to a direct solve of any nonsymmetric rank one perturbation version of the matrix G.

Truncated iterative methods and direct numerical inversions for all the multicomponent transport coefficients have been implemented in the EGlib package [24]. EGlib is a multi-purpose fortran library with scalar and vector optimization and is distributed freely for research purposes. For completeness, several mixture averaged empirical expressions are also included. The package also handles the case of vanishing concentrations by considering rescaled versions of the transport linear systems [8,11].

4 ILLUSTRATION: IMPACT ON COMBUSTION APPLICATIONS

In order to illustrate numerically the theoretical results of the previous sections, we investigate the impact of multicomponent transport on several combustion applications. We focus on the Soret effect arising from the presence of the thermal diffusion ratios in the diffusion velocities. The Soret effect tends to drive light species towards the hot zones of the flow and heavy molecules towards the cold zones. It may thus play a significant role near flame fronts where strong temperature gradients develop. After discussing briefly the numerical methods, we study laminar flame propagation, counterflow flame extinction and multidimensional bunsen flames.

4.1 Numerical model for transport coefficients

In our numerical applications, the collisional cross-sections arising in the transport linear systems have been estimated using the Mason and Monchick approximations [25]. Although the validity of these approximations appears sometimes questionnable in confront to more accurate treatments involving for instance classical or quantal trajectory methods on potential energy surfaces [26,27], they have been retained in the numerical simulations because data is available for all the species relevant to combustion. Collisional cross-sections estimated with more advanced methods can be incorporated in the flame simulations whenever the relevant chemical species have been investigated.

The shear viscosity η is evaluated by considering a system of size n which is symmetric positive definite. An accurate approximation is obtained after one conjugate gradient iteration preconditioned by the matrix diagonal

$$\eta = \frac{\left(\sum_{i\in S} X_i^2/H_{ii}\right)^2}{\sum_{i,j\in S} X_i\, X_j\, H_{ij}/(H_{ii}H_{jj})},$$

where $(H_{ij})_{i,j\in S}$ is the system matrix and X_i the mole fraction of the ith species. For typical mixtures arising in combustion applications, the above expression is at the same time more accurate and cheaper than the Wilke empirical expression. On the other hand, the volume viscosity is neglected in the present work since we only consider low Mach flows where the volume viscosity can be treated as a perturbation of the hydrodynamic pressure.

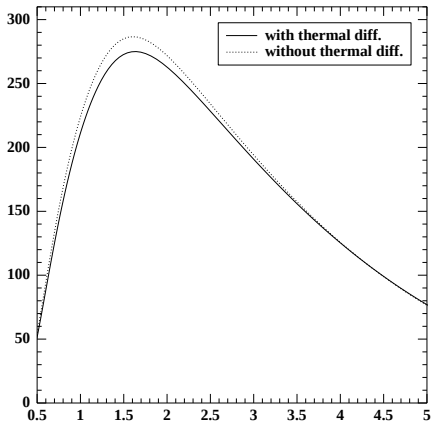

Figure 1. Laminar flame speed (in cm/s) as a function of equivalence ratio.

In order to evaluate the diffusion matrix, we consider the standard transport linear system of size n, often referred to as Stefan-Maxwell-Boltzmann equations, and a projected relaxation method. The first iterate reads

$$D_{[1]} = P\mathrm{diag}(D_{m,i})_{i\in S}P^t$$

where $D_{m,i}$ is a mixture averaged diffusion coefficient of the ith species which can be evaluated from the binary diffusion coefficients [28]. The projector P ensures overall mass conservation, i.e. that the sum of the mass diffusion fluxes is zero. In the results reported below, we consider the second iterate given by

$$D_{[2]} = PZP^t.$$

The matrix Z is dense thus accounting for cross diffusion effects and is detailed in [28].

The thermal conductivity and the thermal diffusion ratios are evaluated from a transport linear system of size n. This system, derived in [29], is obtained by considering basis functions in the variational space $\mathcal{A}$ which only involve the total energy of the molecules instead of separating the translational and internal contributions [4,30,31]. Accurate approximations are obtained by performing three conjugate gradient iterations preconditionned by the matrix diagonal. For more details, we refer to [28,29].

4.2 Impact on laminar flame propagation

Freely propagating laminar flames are obtained experimentally by igniting a fuel and oxydizer mixture inside a tube with negligible heat losses. Under most experimental conditions, a deflagration wave is observed separating fresh from burnt gases. The propagation speed is called the laminar flame speed and only depends on the fresh mixture characteristics. In particular, we are interested in the flame speed as a function of the equivalence ratio Ξ defined by the molar ratio of fuel to oxydizer in the fresh gases. $\Xi = 1$ corresponds to stoichiometric flames, $\Xi > 1$ to rich flames where the fuel is in excess and $\Xi < 1$ to lean flames where the oxydizer is in excess. The governing equations for freely propagating flames express conservation of species mass and temperature in one space dimension and are completed with appropriate boundary conditions [32]. The solution method combines finite difference discretization on locally refined adaptive grids, Newton iterations and a pseudo-arclength continuation procedure [32,33].

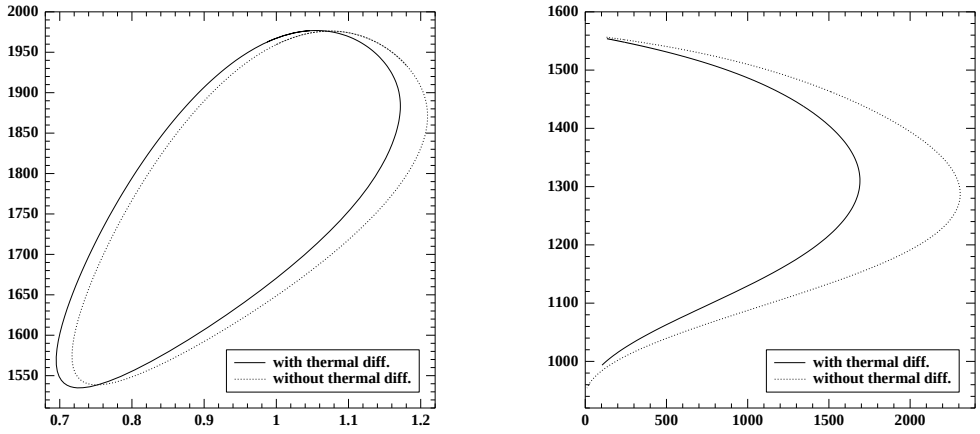

Figure 2. Counterflow flames; left: peak temperature (K) versus equivalence ratio for methane/air flames at a strain rate of 1000 s^{-1}; right: peak temperature (K) versus strain rate for rich hydrogen/air flames with 70 percent hydrogen in mole fraction.

Figure 1 presents the laminar flame speed for hydrogen/air mixtures as a function of equivalence ratio. The results obtained with and without thermal diffusion are compared. We observe that flame speeds are lower with thermal diffusion since active radicals in the reaction zone are less prone to diffuse into the colder ignition zone thus making flame propagation slower. Flame speeds peak for an equivalence ratio of 1.6 where the relative difference between both model predictions is 5%. For very rich flames, flame speeds are slightly higher with thermal diffusion because the thermal diffusion ratio for the O and OH radicals changes sign at the flame front [32].

4.3 Impact on counterflow flame extinction

We consider symmetric counterflow flames in a laminar, stagnation point flow between two opposing premixed jets containing both fuel and oxydizer. This configuration leads to two symmetric counterflow flames. The governing equations expressing conservation of species mass, momentum and energy admit a similarity solution which is given by a boundary value problem in one space dimension [32]. Flame extinction is controlled by two operating parameters: the equivalence ratio and the strain rate imposed on the flame by the stagnation point flow. For a given set of operating parameters, a numerical solution is obtained using the same numerical methods as before.

Numerical results are presented in figure 2. In the left part we consider methane/air flames at a strain rate of 1000 s^{-1} and for various equivalence ratios. Turning points indicate extinction (or flammability) limits with the upper solution branch corresponding to stable solutions and the lower branch to unstable solutions. We observe some differences caused by thermal diffusion in both the lean and rich flammability limits. For instance, the rich flammability limit is $\Xi = 1.21$ when the Soret effect is neglected whereas flames extinguish at $\Xi = 1.17$ when the Soret effect is accounted for. In the right part of figure 2, we consider rich hydrogen/air flames with 70 percent hydrogen in mole fraction for various strain rates. Again, turning points indicate extinction limits. We observe the strong impact of the Soret effect on extinction strain rates which are over 30% lower when the Soret effect is acccounted for.

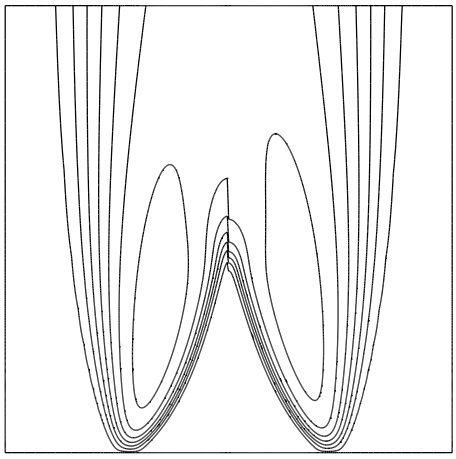

Figure 3. Isotherms between 298 and 1732 K for the lean hydrogen/air bunsen flame; left: with thermal diffusion, right: without thermal diffusion

4.4 Impact on multidimensional bunsen flames

As an illustration for multidimensional flame structures, we consider an axisymmetric hydrogen/air bunsen flame. A lean premixed hydrogen/air mixture is flown through a cylindrical injector. When the jet velocity is larger than the laminar flame speed, a flame of conical shape stabilizes above the lip of the cylindrical burner. The governing equations for bunsen flames express conservation of species mass, momentum and energy in axisymmetric form and are completed with appropriate boundary conditions [28]. A numerical solution is obtained using finite difference discretizations, Newton-Krylov iterations and adaptive gridding techniques.

Isotherms obtained with and without thermal diffusion are presented in figure 3. We observe that the angle at the cone tip is smaller when thermal diffusion is included, as a result of slower flame propagation with thermal diffusion. Thermal diffusion also impacts the spatial distribution of several chemical radicals. For instance, peak values of H and OH along the symmetry axis are respectively a factor of 4 and 2 lower when thermal diffusion is included.

5 CONCLUSIONS

In this paper, we considered a generalized Boltzmann equation valid for dilute, isotropic, polyatomic gas mixtures with chemical reactions. Several chemical regimes have been investigated in the framework of the first order Enskog regime. Two of these regimes are compatible with the H-theorem, the kinetic chemical equilibrium regime and the Maxwellian reaction regime. However, the intermediate regime where the ratio of reactive to inert characteristic times is large but not too much does not yield a positive entropy production. We then reviewed the mathematical properties of the transport linear systems obtained in the Maxwellian reaction regime and presented efficient approximate expressions based on these properties. Finally, the impact of multicomponent transport was illustrated in several combustion applications.

REFERENCES

[1] L. Waldmann und E. Trübenbacher, Formale kinetische Theorie von Gasgemischen aus anregbaren Molekülen, Zeitschr. Naturforschg., 17a (1962) 363–376.

[2] S. Chapman and T.G. Cowling, The Mathematical Theory of Non-Uniform Gases, Cambridge Univ. Press, Cambridge (1970).

[3] J.H. Ferziger and H.G. Kaper, Mathematical Theory of Transport Processes in Gases, North Holland, Amsterdam (1972).

[4] F.R. McCourt, J.J. Beenakker, W.E. Köhler, and I. Kuščer, Non Equilibrium Phenomena in Polyatomic Gases. Volume I: Dilute Gases, Volume II: Cross Sections, Scattering and Rarefied Gases, Clarendon Press, Oxford (1990 and 1991).

[5] G. Ludwig and M. Heil, Boundary layer theory with dissociation and ionization, in Advances in Applied Mechanics, VI, Academic Press, New York (1960) 39–118.

[6] I. Kuščer, Dissociation and recombination in an inhomogeneous gas, Physica A, 176 (1991) 542–556.

[7] C. Grunfeld, On a class of kinetic equations for reacting gas mixtures with multiple collisions, C. R. Acad. Sci. Paris, Série I, 316 (1993) 953–958.

[8] A. Ern and V. Giovangigli, Multicomponent Transport Algorithms, new series monographs vol. m24, Springer, Heidelberg (1994).

[9] B.V. Alexeev, A. Chikhaoui and I.T. Grushin, Application of the generalized Chapman-Enskog method to transport-coefficient calculation in a reacting gas mixture, Phys. Rev. E, 49 (1994) 2809–2825.

[10] A. Ern and V. Giovangigli, The kinetic chemical equilibrium regime, Physica A, 260 (1998) 49–72.

[11] V. Giovangigli, Multicomponent Flow Modeling, Birkhäuser, Boston (1999).

[12] I. Prigogine and E. Xhrouet, On the perturbation of Maxwell distribution function by chemical reactions in gases, Physica, 15 (1949) 913–932.

[13] I. Prigogine and M. Mathieu, Sur la perturbation de la distribution de Maxwell par des réactions chimiques en phase gazeuse, Physica, 16 (1950) 51–64.

[14] K. Takayanagi, On the theory of chemically reacting gas, Prog. Theor. Phys., VI (1951) 486–497.

[15] R.D. Present, On the velocity distribution in a chemically reacting gas, J. Chem. Phys., 31 (1959) 747–750.

[16] B. Shizgal and M. Karplus, Nonequilibrium contributions to the rate of reaction. I. Perturbation of the velocity distribution function, J. Chem. Phys., 52 (1970) 4262–4278.

[17] B. Shizgal and M. Karplus, Nonequilibrium contributions to the rate of reaction. II. Isolated multicomponent systems, J. Chem. Phys., 54 (1971) 4345–4356.

[18] B. Shizgal and M. Karplus, Nonequilibrium contributions to the rate of reaction. III. isothermal multicomponent systems, J. Chem. Phys., 54 (1971) 4357–4362.

[19] A. Ern and V. Giovangigli, Structure of dilute transport linear systems in dilute isotropic gas mixtures, Phys. Rev. E, 53(1) (1996) 485–492.

[20] A. Ern and V. Giovangigli, Fast and accurate multicomponent transport property evaluation, J. Comput. Physics, 120 (1995) 105–116.

[21] S.R. de Groot and P. Mazur, Non-Equilibrium Thermodynamics, Dover, New York (1984).

[22] J.O. Hirschfelder, C.F. Curtiss and R.B. Bird, Molecular Theory of Gases and Liquids, Wiley, New York (1954).
[23] L. Monchick, K.S. Yun and E.A. Mason, Formal kinetic theory of transport phenomena in polyatomic gas mixtures, J. Chem. Phys., 39 (1963) 654–669.
[24] A. Ern and V. Giovangigli, http://www.cmap.polytechnique.fr/www.eglib.
[25] E.A. Mason and L. Monchick, Heat conductivity of polyatomic and polar gases, J. Chem. Phys., 36 (1962) 1622–1639.
[26] V. Vesovic, W.A. Wakeham, A.S. Dickinson, F.R.W. McCourt and M.E. Thachuk, Quantum mechanical calculation of collisional cross-sections for the He-N_2 interaction. II. Thermomagnetic effect, Mol. Phys., 84 (1995) 553–576.
[27] E.L. Heck and A.S. Dickinson, Transport and relaxation cross-sections for pure gases of linear molecules, Comput. Phys. Comm., 95 (1996) 190–220.
[28] A. Ern and V. Giovangigli, Thermal diffusion effects in hydrogen-air and methane-air flames, Combust. Theory Modelling, 2 (1998) 349–372.
[29] A. Ern and V. Giovangigli, Thermal conduction and thermal diffusion in dilute polyatomic gas mixtures, Physica A, 214 (1995) 526–546.
[30] B.J. Thijsse, G.W. 't Hooft, D.A. Coombe, H.F.P. Knaap and J.J.M. Beenakker, Some simplified expressions for the thermal conductivity in an external field, Physica A, 98 (1979) 307–312.
[31] R.J. van den Oord and J. Korving, The thermal conductivity of polyatomic molecules, J. Chem. Phys., 89 (1988) 4333–4338.
[32] A. Ern and V. Giovangigli, Impact of detailed multicomponent transport on planar and counterflow hydrogen/air and methane/air flames, Combust. Sci. Tech., 149 (1999) 157–181.
[33] V. Giovangigli and M.D. Smooke, Adaptive continuation algorithms with application to combustion problems, Appl. Numer. Math., 5 (1989) 305–331.